Vol. 474: 89–104, 2013
doi: 10.3354/meps10107

MARINE ECOLOGY PROGRESS SERIES
Mar Ecol Prog Ser

Published January 31

Snow cover affects ice algal pigment composition in the coastal Arctic Ocean during spring

Eva Alou-Font[1,*], Christopher-John Mundy[1,4], Suzanne Roy[1], Michel Gosselin[1], Susana Agustí[2,3]

[1]Institut des sciences de la mer (ISMER), Université du Québec à Rimouski, 310 Allée des Ursulines, Rimouski, Québec G5L 3A1, Canada

[2]Instituto Mediterráneo de Estudios Avanzados, CSIC-UIB, Miquel Marqués 21, 07190 Esporles, Mallorca, Spain

[3]The UWA Oceans Institute and School of Plant Biology, The University of Western Australia, 35 Stirling Highway, Crawley, 6009 Western Australia, Australia

[4]*Present address:* Centre for Earth Observation Science, Clayton H. Riddell Faculty of Environment, Earth, and Resources, University of Manitoba, Winnipeg, Manitoba R3T 2N2, Canada

ABSTRACT: Specific pigments produced by algae and their degradation products can provide considerable information on the taxonomic composition and photo-physiological state of algal communities. However, no previous study has looked at ice algal pigment composition in the high Arctic. We examined the bottom ice algal pigment composition in the Canadian Beaufort Sea under various snow cover conditions during the spring bloom (March to June 2008). During the early and peak bloom periods, pennate diatoms (pigment Type 2, containing chlorophyll [chl] c_2 and c_3) dominated the chl *a* biomass. Diatoms containing chl c_1 (pigment Type 1) and chlorophytes were only present under high snow cover. A more diverse community was observed during the post-bloom when only low snow cover sites remained due to snow melt, with higher relative contributions of chlorophytes, prasinophytes and dinoflagellates, associated with the loss of diatoms, along with increased abundance of large empty diatoms (from microscopy) and with signs of a deteriorating physiological condition (increases in chlorophyllide *a* and the allomer of chl *a*). The ratio of photoprotective to photosynthetic pigments was generally higher at low snow cover sites, increasing seasonally with the bottom ice irradiance. Low snow cover sites differed also by having more Type 2 diatoms, increased photoprotection and greater chl *a* biomass during the early bloom. In addition, these sites showed increases in chl *a* degradation pigments that may be due to the presence of chlorophyllide-rich pennate diatoms, since the increasing biomass suggests healthy physiological conditions at that time. This study highlights the important influence of light and the light-acclimation plasticity in Arctic sea ice algae.

KEY WORDS: Arctic · Ice algae · Pigments · CHEMTAX · Photoprotection

INTRODUCTION

Sea ice is a major habitat for the microbial community and ice-associated microalgae, generally dominated by pennate diatoms (Poulin et al. 2011). Under-ice light conditions present special problems to cells living in this habitat because photosynthetically active radiation (PAR) is reduced in magnitude. The observed decrease of the sea ice cover over the last 30 yr in the Arctic (NSIDC 2012), together with an earlier ice melt onset in spring and later freeze-up in autumn (Markus et al. 2009), will influence the ice ecosystem; however, the extent of this influence has not yet been determined. Potential impacts include perturbations to the bottom ice light environment, where the majority of ice algal biomass can be

*Email: eva_alou@yahoo.com

observed in the Canadian Arctic (Smith et al. 1990). The bottom ice light regime in the Arctic is strongly affected not only by the ice but also by the snow cover (Mundy et al. 2005). While ice thickness decreases as spring progresses, most of the spatial variability in bottom ice irradiance is due to snow depth and melt pond coverage (Perovich et al. 1998). With melting of the snow and sea ice cover, ice algae are exposed to increases in irradiance, including ultraviolet radiation which has been shown to penetrate sea ice (Belzile et al. 2000). If the amount of light absorbed exceeds the capacity for utilization by photochemistry, photodamage can occur, especially at low temperatures that could enhance the sensitivity of cells (Huner et al. 1998). A recent study suggested that photodamage of cells during high irradiance exposure controls phytoplankton growth in the Southern Ocean rather than the low levels of light or inadequate iron supply (Alderkamp et al. 2010). However, examination of the photoprotective mechanisms employed by bottom sea ice algae from Antarctica indicated that these algae possess a high level of plasticity in their light acclimation capabilities, notably due to an active xanthophyll cycle associated with non-photochemical quenching of chlorophyll fluorescence which reduces the excitation pressure on Photosystem II (Petrou et al. 2011). The degree of plasticity in light acclimation has been suggested to explain the changes in algal community in the Antarctic (Arrigo et al. 2010, Petrou & Ralph 2011) and the Arctic (Ban et al. 2006).

Since timing and rate of loss of the ice and snow cover determine the degree of photo-physiological stress in ice algae, it is important to know how changes in the light regime might affect the sea ice community. In the present work, we focus on the influence of the snow cover on the community composition and pigment-related photoprotective response of ice algae during the sea ice diatom bloom and secondarily examine the changes that take place as this bloom progresses. The main objectives were to (1) determine if ice algal taxonomic composition was different under the various snow cover conditions and periods of the bloom, (2) investigate the photoprotective response of communities of ice algae under 3 contrasting snow cover conditions (low, mid and high snow depths) and (3) determine if cells exposed to higher irradiances (low snow cover depth) showed a detrimental physiological condition. In order to study changes in the taxonomic composition of the major algal groups we used chemo-taxonomy (CHEMTAX factorization, Mackey et al. 1996) on high-performance liquid chromatography (HPLC) pigment signatures with confirmation from microscopy. CHEMTAX factorization has been used successfully in polar waters (Ishikawa et al. 2002, Wright et al. 2010), but no study has yet been done for Arctic sea ice.

MATERIALS AND METHODS

Study site and sampling

This study was conducted in the Canadian Beaufort Sea (Fig. 1) as part of the International Polar Year–Circumpolar Flaw Lead system study (IPY–CFL; Barber et al. 2010), onboard the Canadian Coast Guard Ship (CCGS) 'Amundsen'. Sampling was carried out on 27 separate days from 18 March to 22 June 2008 on first-year drifting sea ice ('D' stations) of the Amundsen Gulf and on the first-year landfast ice ('F' stations) of Franklin and Darnley Bays, Prince of Wales Strait and M'Clure Strait's entrance (northwestern Banks Island) (Fig. 1).

Downwelling PAR (400 to 700 nm) incident irradiance was continuously monitored (PARLite™

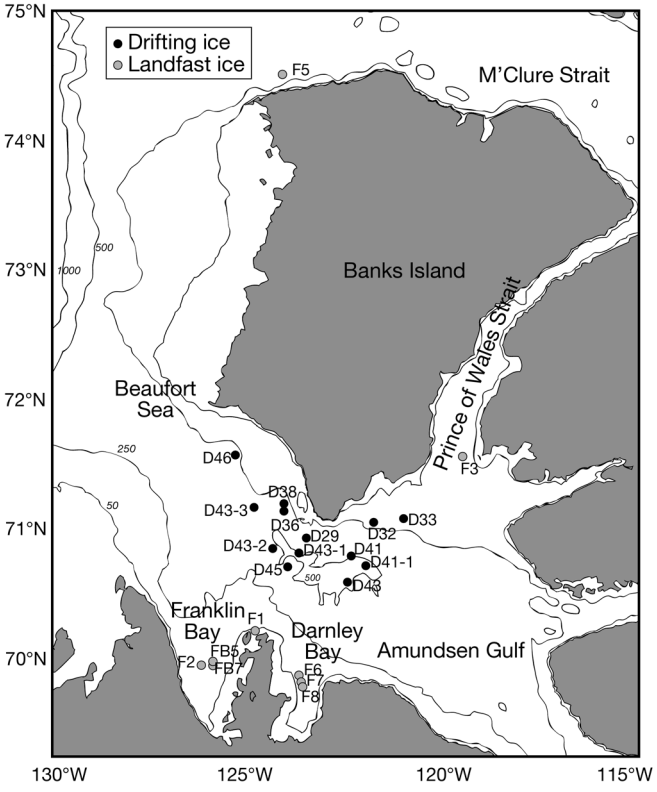

Fig. 1. Locations of sampling stations in the Canadian Beaufort Sea during the International Polar Year-Circumpolar Flaw Lead system study, March to June 2008. Water depth is in meters

quantum sensor, Kipp & Zonen) on a tower at the bow of the ship commencing on 1 April. PAR values were integrated to obtain daily incident PAR. PAR downwelling incident irradiance was also measured at every sampling site (between 09:00 and 11:00 h) at the surface (E_0) and at the ice–water interface (E_s), using Li-Cor 2π sensors (LI-190SA quantum and LI-192SA underwater quantum sensors) between 26 April and 2 June. Sub-ice measurements were taken using an under-ice arm as described in Mundy et al. (2007). Irradiance reaching the top of the bottom 3 cm algal layer (bottom ice irradiance, E_b in µmol photons m^{-2} s^{-1}) was estimated from that at the ice–water interface, using Beer's law (details provided in Supplements 1 & 2 at www.int-res.com/articles/suppl/m474p089_supp.pdf). The percent transmission of incident irradiance reaching the top of the bottom ice algal layer was defined as $\%E_b = (E_b/E_0) \times 100$. The $\%E_b$ was multiplied by the daily incident irradiance, then averaged over 3 d leading up to the sample collection date in order to determine the mean irradiance received by bottom ice algae.

Routine ice sampling was performed at low (<5 cm), medium (8 to 15 cm), or high (>15 cm) snow depth sites until 20 May. Afterwards, only low snow cover sites remained to be sampled due to snow melting. Sampling sites for the different snow cover conditions were within close proximity of each other at the various stations (<30 m apart). Bottom ice cores (3 cm) were collected with a Mark II ice corer (9 cm internal diameter, Kovacs Enterprises). Snow depth and ice thickness were measured at each core location. Bottom ice cores used for bulk ice salinity and nutrient measurements were extracted and melted slowly in the dark in sterile bags (Nasco Whirl-Pak®). For biological measurements, 4 to 5 replicate ice cores were extracted and pooled in a single dark isothermal container. Melting was done overnight in a variable volume (1.2 to 3.5 l) of 0.2 µm filtered surface seawater to minimize osmotic stress on the ice algae (Garrison & Buck 1986).

Salinity and nutrients

A WTW 330i conductivity meter was used to determine salinity of the bottom ice samples. Nitrate plus nitrite (NO_3 + NO_2), nitrite (NO_2), silicic acid [$Si(OH)_4$] and phosphate (PO_4) were determined on board the ship with a Bran-Luebbe III nutrient autoanalyzer (adapted from Grasshoff et al. 1999). Prior to nutrient analysis, samples were filtered through precombusted Whatman GF/F filters. Nutrient concentrations were corrected for the influence of salinity using a simple linear correction (Grasshoff et al. 1999).

Microscopic analysis

Samples for microscopic analysis were preserved with acidic Lugol's solution and stored in the dark at 4°C until analysis. Cells >2 µm were identified using an inverted light microscope (WILD Heerbrugg). A minimum of 400 cells were enumerated over at least 3 transects. Detailed taxonomic analysis will be presented elsewhere (Mundy et al. 2011, Philippe in press), but the abundance of the major algal groups is shown below.

Pigment analysis using HPLC

The identity and concentration of algal pigments were determined by reverse-phase HPLC. Samples were filtered onto 25 mm Whatman GF/F filters (maximum volume of 500 ml and maximum time of filtration of 20 min). The samples were immediately placed in liquid nitrogen over at least a 24 h period, and then transferred to a −80°C freezer on board the ship. Samples were sent every 6 wk by plane to Rimouski in a liquid nitrogen dry-shipper, and thereafter were kept in a −80°C freezer until analysis. Algal pigments were extracted in 95% methanol, sonicated (Sonicator Ultrasonic Processor XL 2010) for 15 s on ice and centrifuged for 5 min at 3700 × *g*. Extracts were filtered through a 0.22 µm polytetrafluoroethylene syringe filter and poured in an autosampler vial which was gently sparged with argon to limit oxidation. A volume of 50 µl was injected in a Waters Symmetry C8 column (150 × 4.6 mm, 3.5 µm). Gradient elution was controlled by a Thermo Separation (TSP) P4000 pump with solvents as indicated in Zapata et al. (2000). Pigments were detected with a TSP UV 6000 LP diode-array absorbance detector (400 to 700 nm) and a TSP FL3000 fluorescence detector to confirm the presence of chlorophyll-related compounds. Calibration was done with external pigment standards obtained from DHI Water & Environment (Hørsholm, Denmark), and extinction coefficients were taken from Jeffrey (1997). Limits of detection and quantification were estimated as in Bidigare et al. (2005), and pigments with concentrations below the limit of detection were not reported. Marker pigments were identified through comparison with the retention time and spectral properties of

pigment standards. A pigment-based index of diversity was calculated using the formula

$$(1/n)\Sigma - n_i(\log n_i - \log n)$$

where n is the total concentration of all marker pigments (chlorophyll *a* [chl *a*] excluded) and n_i is the concentration of each specific marker pigment (Shannon 1948, see Roy et al. 2006).

CHEMTAX analysis

The contribution of major algal groups to total chl *a* was determined using the CHEMTAX software (Mackey et al. 1996, Version 1.95 as used in Wright et al. 2009) with confirmation from the microscopic analysis. This new version of the software sets up multiple (60) initial pigment ratio matrices and directs the program to use each of them in turn to obtain more stable final values ('successive runs' strategy, as recommended by Latasa 2007). Since CHEMTAX should be applied to data sets with stable pigment ratios (Mackey et al. 1996), samples were separated into 5 data sets with similar environmental (snow depth) and biological (algal bloom phase) conditions. For the early bloom period, we split the samples into 3 groups: (1) low (n = 10 samples), (2) mid (n = 7) and (3) high (n = 9) snow cover depths. Initial pigment ratios for these 3 groups differed according to irradiance (e.g. low light pigment ratios for high snow cover and higher light pigment ratios for low snow cover conditions), with pigment ratios taken from the polar literature given below or from Higgins et al. (2011). The fourth data set was the peak bloom period (n = 14 samples), with similar pigment ratios under all snow covers, and the last was the post-bloom period (n = 11 samples). CHEMTAX was used separately on each data set. The initial pigment ratio matrices were based on previous CHEMTAX analyses from polar water studies (Mackey et al. 1996, Ishikawa et al. 2002, Rodriguez et al. 2002, Suzuki et al. 2002, Wright et al. 2010, Higgins et al. 2011, Kozlowski et al. 2011).

Statistical analyses

Kruskal-Wallis test, Mann-Whitney *U*-test and Wilcoxon's signed-rank test were performed to seek differences among snow cover depths or sampling periods. Descriptive statistics, Spearman's rank order correlations (r_s) and Pearson's linear regressions were obtained using SigmaStat 3.5 and SigmaPlot 10.0 (Systat Software).

RESULTS

Algal biomass

As observed in previous studies from the Canadian Arctic, ice algal biomass increased from March until early May and decreased in June (Fig. 2). The early bloom period lasted from 18 March to 19 April, with chl *a* concentrations ranging from <0.01 to 14 mg m^{-2}, followed by the peak bloom period from 26 April to 16 May (10 to 100 mg chl *a* m^{-2}). The post-bloom period took place in the second half of May and in June, with much lower concentrations of chl *a*, reaching a minimum of 0.02 mg m^{-2} at Stn F8. Maximum chl *a* concentrations found in this study were up to 3 times higher than what has been observed in the past (30 to 31 mg m^{-2}; Różańska et al. 2009). These high values have been attributed to enhanced under-ice nutrient availability due to wind-driven upwelling events (Tremblay et al. 2011). During the early bloom period, chl *a* concentrations were significantly higher for the low snow (mean ± SD: 4.7 ± 4.9 mg m^{-2}) than

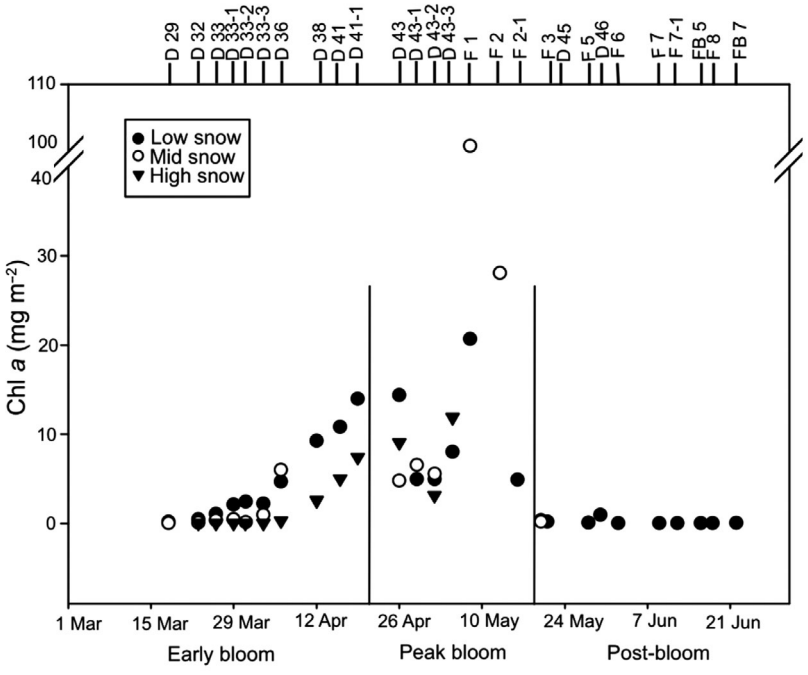

Fig. 2. Temporal change in chlorophyll *a* (chl *a*) concentration during the 3 bloom periods under low, mid and high snow cover conditions. Sampling stations shown in Fig. 1 are indicated at the top of this figure

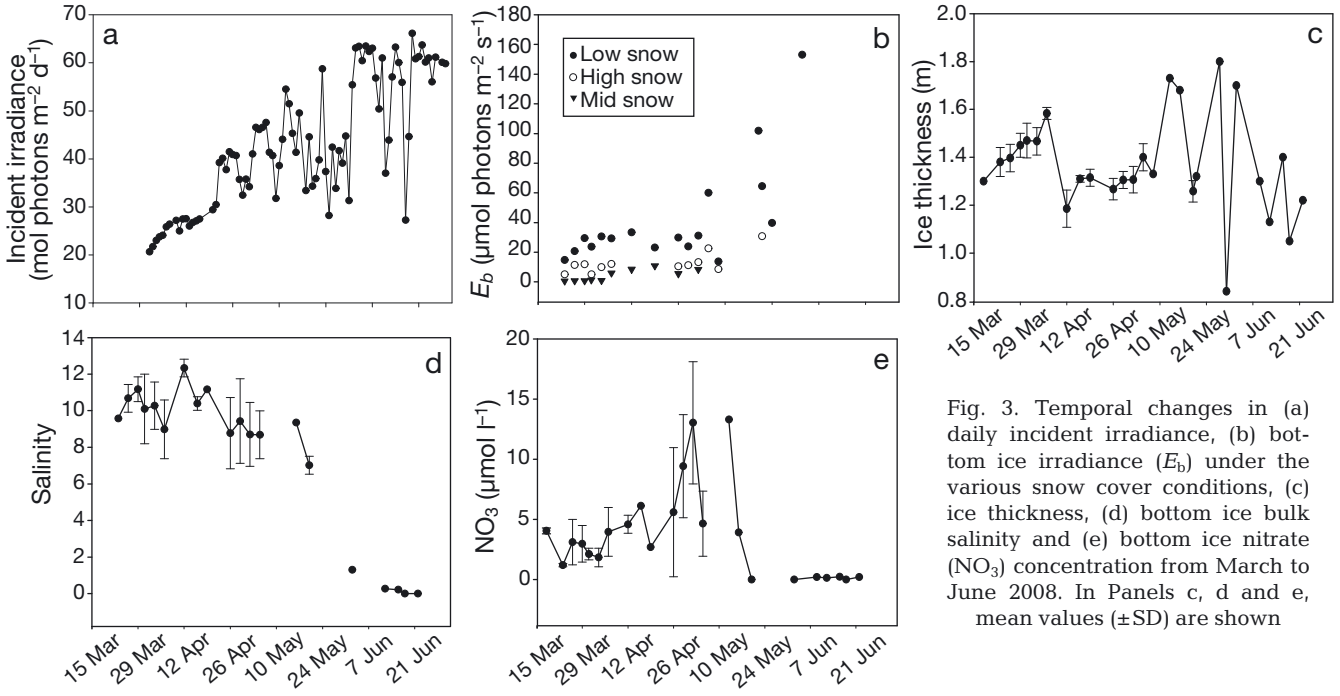

Fig. 3. Temporal changes in (a) daily incident irradiance, (b) bottom ice irradiance (E_b) under the various snow cover conditions, (c) ice thickness, (d) bottom ice bulk salinity and (e) bottom ice nitrate (NO_3) concentration from March to June 2008. In Panels c, d and e, mean values (±SD) are shown

for the mid (1.2 ± 2.2 mg m^{-2}) or high (1.7 ± 2.8 mg m^{-2}) snow cover conditions (Kruskal-Wallis test, $p < 0.05$). However, no significant difference in chl *a* between snow cover conditions was observed during the peak bloom period (Kruskal-Wallis test, $p > 0.05$).

Light and chemical variables

Incident daily PAR increased seasonally, from 20.6 mol photons m^{-2} d^{-1} on 1 April to 66.9 mol photons m^{-2} d^{-1} on 18 June (Fig. 3a). Bottom ice irradiance (E_b) differed among the snow cover conditions during the early bloom (Fig. 3b), with significantly higher values for low snow (E_b and $\%E_b$ [mean ± SD] = 25.6 ± 6.2 µmol photons m^{-2} s^{-1}, 11.2 ± 3.6%, respectively) than for mid (9.2 ± 3.3 µmol photons m^{-2} s^{-1}, 4.5 ± 1.6%), or high snow cover conditions (3.7 ± 4.1 µmol photons m^{-2} s^{-1}, 1.0 ± 1.1%) during the early bloom (Kruskal-Wallis test, $p < 0.05$). During the peak bloom, after the removal of an outlier (Stn F2, assumed to be a measurement error), E_b showed less variability between snow cover conditions. However, it was still significantly higher under low snow (43.4 ± 32.6 µmol photons m^{-2} s^{-1}, 4.0 ± 3.1%) than under mid (13.2 ± 5.5 µmol photons m^{-2} s^{-1}, 1.2 ± 0.4%) or high snow cover conditions (7.0± 2.0 µmol photons m^{-2} s^{-1}, 0.7 ± 0.3%; Wilcoxon's signed-rank tests, $p < 0.05$). During the post-bloom, E_b increased to a maximum value of 153.1 µmol photons m^{-2} s^{-1} (12.3%) observed at Stn F6. Unfortunately, sub-ice irradiances (E_s) used to estimate E_b were not measured after 2 June and high and mid snow conditions had all but disappeared by that time, due to snow melting.

The average sea ice thickness was about 1.3 m (Fig. 3c), and it did not differ significantly among the bloom periods, although it decreased during the post-bloom, reaching a minimum on 30 May (0.8 m, Stn D46). No significant difference in sea ice thickness was observed between the different snow cover conditions during the early bloom and peak bloom periods (Kruskal-Wallis tests, $p > 0.05$).

Bottom bulk ice salinity (Fig. 3d) averaged (± SD) 10.4 ± 1.3 for the early bloom and 9.0 ± 1.5 for the peak bloom, remaining relatively constant during these 2 periods, but decreased to a value of 3.0 ± 3.2 during the post-bloom period (Kruskal-Wallis test, $p < 0.05$). There were no significant differences in salinity among the snow cover conditions for the early bloom and peak bloom periods.

Over the entire study, the concentrations of NO_3 ranged from <0.05 to 18.9 µmol l^{-1} (Fig. 3e), $Si(OH)_4$ from <0.2 to 22.5 µmol l^{-1} and PO_4 from <0.02 to 4.2 µmol l^{-1}. There were no significant differences among snow cover conditions, except for PO_4 during the early bloom, which showed greater concentrations under low snow cover (data not shown, Kruskal-Wallis test, $p < 0.05$). NO_3 averaged (± SD) 3.1 ± 1.6 µmol l^{-1} for the early bloom, 8.4 ± 5.3 µmol l^{-1} during the peak bloom (increase due to local upwelling: Tremblay et al. 2011) and 0.1 ± 0.1 µmol l^{-1} during the

post-bloom period. $Si(OH)_4$, PO_4 and NO_3 concentrations were all significantly lower during post-bloom (Mann-Whitney *U*-test, $p < 0.01$). The NO_3:PO_4 and NO_3:$Si(OH)_4$ molar ratios decreased throughout the study and were lower than the critical values of 16 for NO_3:PO_4 (Redfield et al. 1963) and of 1.1 for NO_3:$Si(OH)_4$ (Brzezinski 1985), suggesting that nitrogen was the limiting nutrient for algal growth.

Pigment composition and distribution

The pigments determined with HPLC and used in the initial matrix for the CHEMTAX analyses included the chlorophylls *a*, *b*, c_1, c_2 and c_3, Mg-2,4-divinyl pheoporphyrin a_5 monomethyl ester (MgDVP) and the carotenoids peridinin, fucoxanthin, neoxanthin, violaxanthin, alloxanthin, lutein and zeaxanthin. Pigments representing <0.01 mg m^{-2} or having sporadic presence were not considered.

The relative concentration of the major marker pigments is presented in Fig. 4. Fucoxanthin dominated, with 61 and 65% of the sum of accessory pigments during the early and peak bloom periods, respectively. The temporal distribution of fucoxanthin displayed the same trend as chl *a*, with which it was strongly correlated ($r_s = 0.99$, $p < 0.0001$, $n = 27$). This suggests a high contribution of diatoms to the total algal biomass, which was confirmed by microscopy and the CHEMTAX analyses (see following subsection). Chl c_2 was the pigment with the next highest relative concentration (12 to 16%; Fig. 4). During the post-bloom period, the decrease in relative concentrations of fucoxanthin and chl c_2 was accompanied by an increase in other accessory pigments, such as chl *b* (present in chlorophytes and prasinophytes) and peridinin (present in some dinoflagellates). We did not detect any pigments specific to haptophytes (such as 19′-hexanoyloxyfucoxanthin). Microscopic observations confirmed that this group was scarcely present. Therefore, we attributed the presence of fucoxanthin to diatoms throughout our study.

Relative contribution of taxonomic groups (CHEMTAX and microscopy)

An example of the initial marker pigment to chl *a* ratios (wt:wt) for the various algal groups considered and of the final ratios after optimization by CHEMTAX is presented in Tables 1 & 2 (see Supplement 1 for remaining ratios). These ratios were used to calculate the relative contribution of each sea ice algal

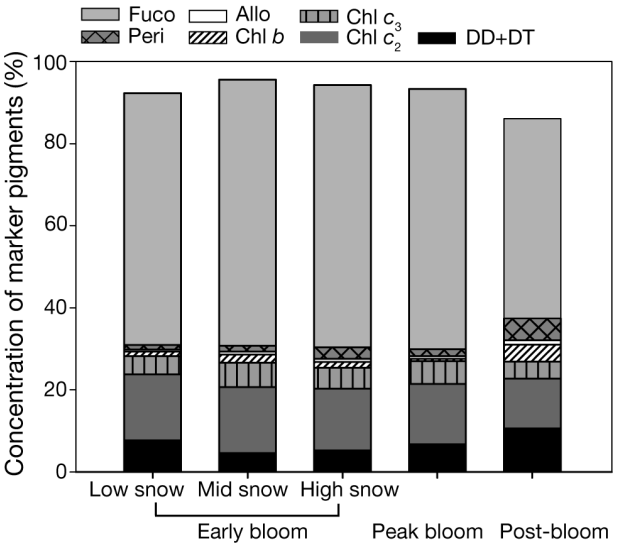

Fig. 4. Mean relative concentration of the main marker pigments to total accessory pigments (wt:wt) under different snow cover conditions during the early bloom and under all snow covers together during the peak bloom and post-bloom periods. The coefficients of variation for individual pigments ranged between 2 and 36%. DD+DT: sum of diadinoxanthin and diatoxanthin. See Table 1 for other pigment abbreviations

group to total chl *a* (Figs. 5a,b,c & 6a,b). Some of these groups (e.g. diatoms, dinoflagellates) possess several pigment-based algal types; the most recent description of these can be found in Jeffrey et al. (2011). In general, the final pigment ratios differed little from the starting literature values and were within the ranges of these values with only a few exceptions. During the early bloom, for the mid snow cover conditions, the ratio of alloxanthin to chl *a* for cryptophytes decreased from 0.253 (initial ratio) to 0.061 (final CHEMTAX ratio), this value being somewhat lower than the minimum value found in the literature (0.104; Higgins et al. 2011). For the same period and snow cover conditions, the chl *b* attributed to prasinophytes Type 2 showed an increase in its ratio to chl *a* from 0.786 to 1.116. This last value is only slightly higher than that reported by Rodriguez et al. (2002) for the prasinophyte *Pyramimonas* spp. (0.977). During the peak bloom period, the ratio of fucoxanthin to chl *a* for diatoms Type 2 increased from 1.1 to 1.5, close to the maximum value found in Suzuki et al. (2002) (1.4) or in Higgins et al. (2011) (1.3).

Most of the CHEMTAX-identified diatoms belonged to pigment Type 2 (Higgins et al. 2011), which contains fucoxanthin and chl c_2 and c_3. These were likely associated with pennate diatoms as observed microscopically. Cryptophytes (with alloxanthin as diagnostic pigment) were present according to

Table 1. Example of initial pigment to chlorophyll (chl) *a* ratios for each algal group encountered in the sea ice as used for CHEMTAX calculations and final ratios after optimization by CHEMTAX. Matrices are shown here for the low snow cover conditions during early bloom. β,β-carotene was not included in the CHEMTAX analyses since it is ambiguous as a biomarker (present in several algal groups). MgDVP: Mg-2,4-divinyl pheoporphyrin a_5 monomethyl ester; Peri: peridinin; Fuco: fucoxanthin; Neo: neoxanthin; Viola: violaxanthin; Allo: alloxanthin; Prasino2: prasinophytes Type 2; Dino1: dinoflagellates Type 1; Crypto: cryptophytes; Chloro: chlorophytes; Diatom2: diatoms Type 2

	Chl c_3	Chl c_2	Chl c_1	MgDVP	Peri	Fuco	Neo	Viola	Allo	Chl *b*	Chl *a*
Initial ratio matrix – early bloom and low snow cover											
Prasino2	0	0		0.023	0	0	0.056	0.055	0	0.786	1
Dino1	0	0.162		0.004	0.675	0	0	0	0	0	1
Crypto	0	0.204		0	0	0	0	0	0.253	0	1
Diatom2	0.066	0.299		0	0	0.755	0	0	0	0	1
Output ratio matrix – early bloom and low snow cover											
Prasino2	0	0		0.025	0	0	0.048	0.067	0	0.532	1
Dino1	0	0.138		0.004	0.467	0	0	0	0	0	1
Crypto	0	0.173		0	0	0	0	0	0.129	0	1
Diatom2	0.032	0.109		0	0	0.504	0	0	0	0	1

Table 2. Example of initial pigment to chlorophyll (chl) *a* ratios for each algal group encountered in the sea ice as used for CHEMTAX calculations and final ratios after optimization by CHEMTAX. Matrices are shown here for all snow covers during the post-bloom. As in Table 1, β,β-carotene was not included. Zea: zeaxanthin; Lut: lutein; Chloro: chlorophytes; see Table 1 for other abbreviations

	Chl c_3	Chl c_2	Chl c_1	MgDVP	Peri	Fuco	Neo	Viola	Allo	Zea	Lut	Chl *b*	Chl *a*
Initial ratio matrix – post-bloom													
Prasino2	0	0		0.023	0	0	0.120	0.160	0	0	0.009	0.945	1
Dino1	0	0.300		0.008	1.063	0	0	0	0	0	0	0	1
Crypto	0	0.200		0	0	0	0	0	0.229	0	0	0	1
Chloro	0	0		0	0	0	0.020	0.040	0	0.009	0.203	0.263	1
Diatom2	0.066	0.299		0	0	0.755	0	0	0	0	0	0	1
Output ratio matrix – post-bloom													
Prasino2	0	0		0.026	0	0	0.125	0.200	0	0	0.009	0.810	1
Dino1	0	0.350		0.010	1.352	0	0	0	0	0	0	0	1
Crypto	0	0.183		0	0	0	0	0	0.223	0	0	0	1
Chloro	0	0		0	0	0	0.018	0.050	0	0.010	0.176	0.093	1
Diatom2	0.068	0.116		0	0	0.682	0	0	0	0	0	0	1

CHEMTAX and also observed microscopically (*Rhodomonas baltica*). Peridinin-containing dinoflagellates (labeled Type 1 in Higgins et al. 2011) likely included the genus *Amphidinium*, also observed during the present study. The prasinophytes present (designated Type 2 in the present study and Type 2A in Higgins et al. 2011) lacked prasinoxanthin and may have included species from the genus *Pyramimonas*, which were observed by microscopy in the present study, as in that of Różańska et al. (2009).

Relative contributions of the various algal groups showed that diatoms were already dominant in early bloom under all snow cover conditions, ranging from 40 to 90% for both CHEMTAX (Fig. 5a,b,c) and microscopy (Fig. 5d). Cryptophytes were the second major group (2 to 37%), followed by generally smaller contributions from prasinophytes (2 to 29%) and dinoflagellates (1 to 12%), according to CHEMTAX. For microscopy, groups other than diatoms represented from 1 to 32% of the total number of cells (Fig. 5d).

Relative contributions of the various algal groups resulting from CHEMTAX showed some differences among the 3 snow cover conditions (Fig. 5a,b). For the group of Stns D32 to D36 (studied under the 3 snow cover conditions), we observed a higher percentage of prasinophytes (5 ± 12%) and cryptophytes (19 ± 17%) under high snow conditions than for low (prasinophytes: 3 ± 2%, cryptophytes: 8 ± 10%) or mid snow cover conditions (prasinophytes: 3 ± 1%, cryptophytes: 13 ± 7%), respectively. However, these differences were not significant (Kruskal-Wallis test,

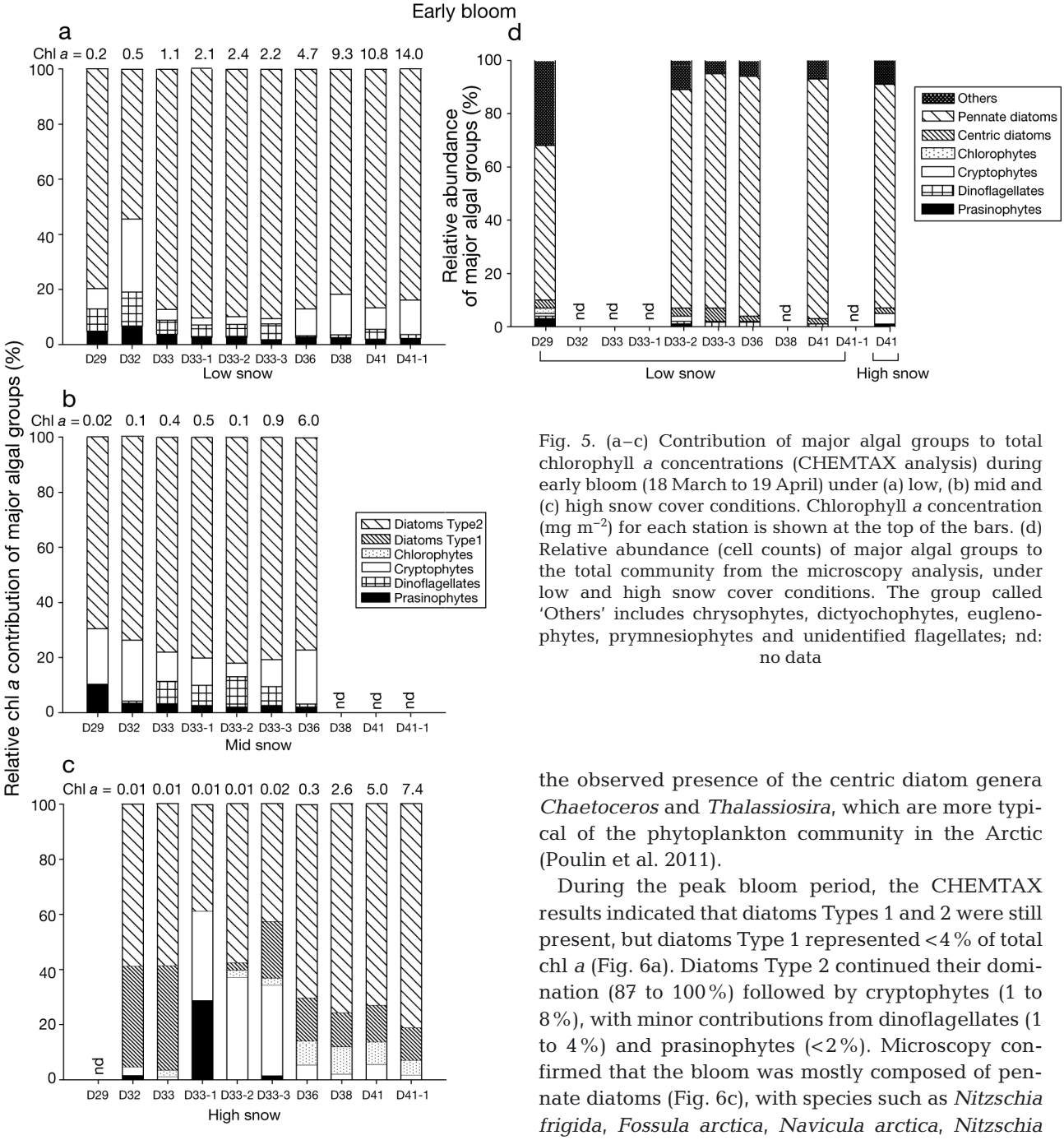

Fig. 5. (a–c) Contribution of major algal groups to total chlorophyll *a* concentrations (CHEMTAX analysis) during early bloom (18 March to 19 April) under (a) low, (b) mid and (c) high snow cover conditions. Chlorophyll *a* concentration (mg m^{-2}) for each station is shown at the top of the bars. (d) Relative abundance (cell counts) of major algal groups to the total community from the microscopy analysis, under low and high snow cover conditions. The group called 'Others' includes chrysophytes, dictyochophytes, euglenophytes, prymnesiophytes and unidentified flagellates; nd: no data

$p > 0.05$). Only the percentage of diatoms Type 2 was significantly lower for high snow cover (54 ± 2%) than for low (83 ± 14%) or mid (78 ± 3%) snow cover conditions (Kruskal-Wallis test, $p < 0.05$). The communities present under the high snow cover were also distinguished by the absence of dinoflagellates, the presence of chl *b*-containing chlorophytes, matching with *Dunaliella* spp. (observed by microscopy), and the presence of a second type of diatoms (Type 1; Higgins et al. 2011), characterized by the presence of chl c_1. This second type was likely associated with the observed presence of the centric diatom genera *Chaetoceros* and *Thalassiosira*, which are more typical of the phytoplankton community in the Arctic (Poulin et al. 2011).

During the peak bloom period, the CHEMTAX results indicated that diatoms Types 1 and 2 were still present, but diatoms Type 1 represented <4% of total chl *a* (Fig. 6a). Diatoms Type 2 continued their domination (87 to 100%) followed by cryptophytes (1 to 8%), with minor contributions from dinoflagellates (1 to 4%) and prasinophytes (<2%). Microscopy confirmed that the bloom was mostly composed of pennate diatoms (Fig. 6c), with species such as *Nitzschia frigida*, *Fossula arctica*, *Navicula arctica*, *Nitzschia promare*, *Navicula* sp. and *Entomoneis* sp., along with a few centric diatoms such as *Attheya septentrionalis*. There were no differences among snow cover conditions during this period.

Community composition was more variable during the post-bloom period, along with a strong decline of the algal biomass. Microscopy results showed a growing importance of groups other than diatoms for this period (average [± SD] for these other groups = 32 ± 19%), mostly due to unidentified flagellates. The relative contribution of diatoms (CHEMTAX) was

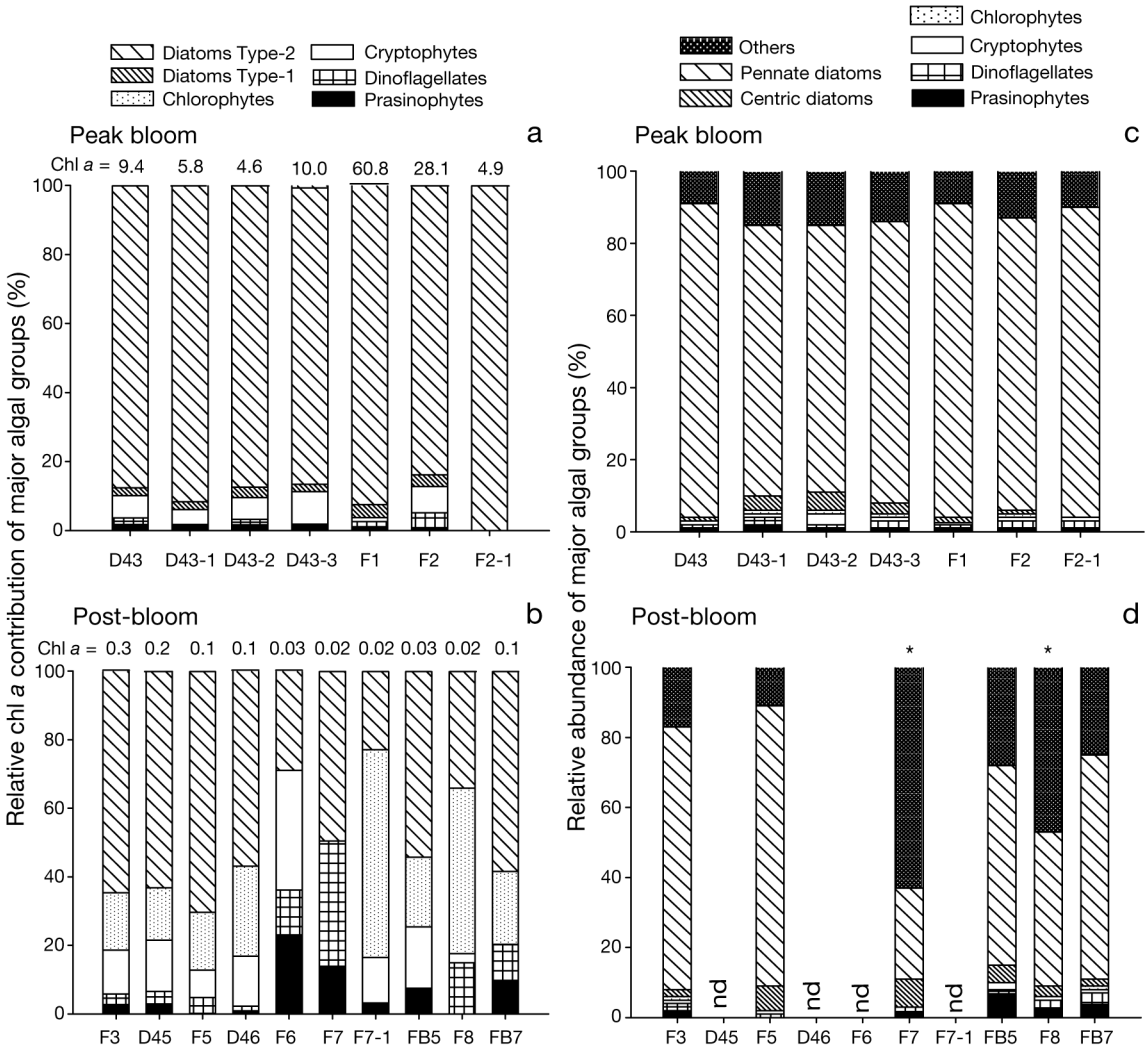

Fig. 6. Same as Fig. 5, but for the peak bloom (a,c) and post-bloom periods (b,d). (a,b) pigment-based contribution of major algal groups to total chlorophyll (chl) *a* concentrations (CHEMTAX analysis). (c,d) relative abundance of major algal groups (microscopy analyses). Chl *a* concentration (mg m^{-2}) for each station is shown at the top of the bars. For Stns D43, D43-1, D43-2, D43-3, F1 and F3, chl *a* values are averages over the different snow cover conditions. For microscopy, the group called 'Others' includes chrysophytes, dictyochophytes, euglenophytes, prymnesiophytes and unidentified flagellates. In (d) asterisks above 2 bars indicate that microscopically unidentified flagellates (2 to 20 µm) represented a large proportion of the total community at those stations; nd: no data

also significantly lower than in the 2 previous periods (Kruskal-Wallis test, $p < 0.001$). Dinoflagellates ranged from <1 to 37%, and cryptophytes, from <1 to 35%, with trends generally opposite to those of dinoflagellates. The maximum contribution of chlorophytes was found at Stn F7-1 (61%), but this group was absent from Stns F6 and F7. Prasinophytes were also present, with a maximum of 23% at Stn F6 (Fig. 6b).

The pigment-based diversity index of the community was lowest at the peak of the bloom and it was highest during the post-bloom period (Table 3). During the early bloom and peak bloom, the communities under the low, mid and high snow cover conditions showed generally similar diversity.

Photosynthetic (PSC) and photoprotective (PPC) carotenoids

The highest concentrations of chl *a*, PSC (sum of fucoxanthin, peridinin, neoxanthin and alloxanthin) and PPC (sum of diadinoxanthin, diatoxanthin, violaxanthin, zeaxanthin, lutein and β,β-carotene) were observed during the peak bloom period, under mid snow cover conditions at Stns F1 near Cape Parry

(54.0 mg PSC m^{-2} and 6.4 mg PPC m^{-2}) and F2 in Franklin Bay (13.0 mg PSC m^{-2} and 2.0 mg PPC m^{-2}). All other stations had much lower concentrations. High PPC concentrations were mostly due to the presence of diadinoxanthin (DD), β,β-carotene and diatoxanthin (DT) with an average contribution to total PPC of 57, 23 and 18%, respectively.

The PPC:PSC ratio increased seasonally (Fig. 7a) as downwelling incident irradiance increased (Fig. 3a). Irradiance clearly influenced this response, with a PPC:PSC ratio varying from 0.13 to 0.45 (wt:wt) at stations with daily incident irradiance <50 mol photons m^{-2} and from 0.97 to 3.50 for the stations exposed to higher daily incident irradiance (during post-bloom).

The PPC:PSC ratio was also significantly higher under low snow (mean ± SD: 0.19 ± 0.03, Mann-Whitney *U*-test, $p < 0.05$) than under mid or high snow cover conditions during the early bloom. This was also the case during the peak bloom period (low snow cover condition: 0.20 ± 0.02, Mann-Whitney *U*-test, $p < 0.01$), indicating a response to the (also significantly) higher transmitted irradiance under low snow cover conditions during these 2 periods (Fig. 3b).

Similar trends were observed with the main diatom xanthophyll cycle pigments (DD + DT). The (DD + DT):chl *a* ratio increased over time (Fig. 7b), paralleling the seasonal increase in daily incident irradiance ($r_s = 0.70$, $p < 0.001$; Fig. 3a). Values were significantly higher (Mann-Whitney *U*-test, $p < 0.001$) for stations with daily incident irradiance >50 mol photons m^{-2}, with a maximum (DD + DT):chl *a* value of 0.70 for Stn F8. As for PPC:PSC, there was no difference in (DD + DT):chl *a* between the mid or high snow cover conditions, but this ratio was significantly higher under low snow (Mann-Whitney *U*-tests, $p < 0.01$, after removal of 2 outliers at Stns D33-1 and D33-2, which had concentrations of chl *a* and DT ≤ 0.01 mg m^{-2}). The increase in irradiance between high and mid snow cover conditions was likely insufficient to elicit a response in terms of photoprotective pigments. The level of deepoxidation or relative fraction of DT, i.e.

Table 3. Mean (SD in parentheses) pigment-based index of diversity under different snow cover conditions during the early bloom (18 March to 19 April), peak bloom (26 April to 16 May) and post-bloom periods (20 May to 22 June); n: number of observations; n.d.: no data

Stage	Snow cover		
	Low	Mid	High
Early bloom	0.24 (0.09) n = 10	0.20 (0.03) n = 7	0.29 (0.08) n = 9
Peak bloom	0.15 (0.02) n = 6	0.15 (0.02) n = 5	0.18 (0.03) n = 3
Post-bloom	0.40 (0.12) n = 10	0.57 n = 1	n.d.

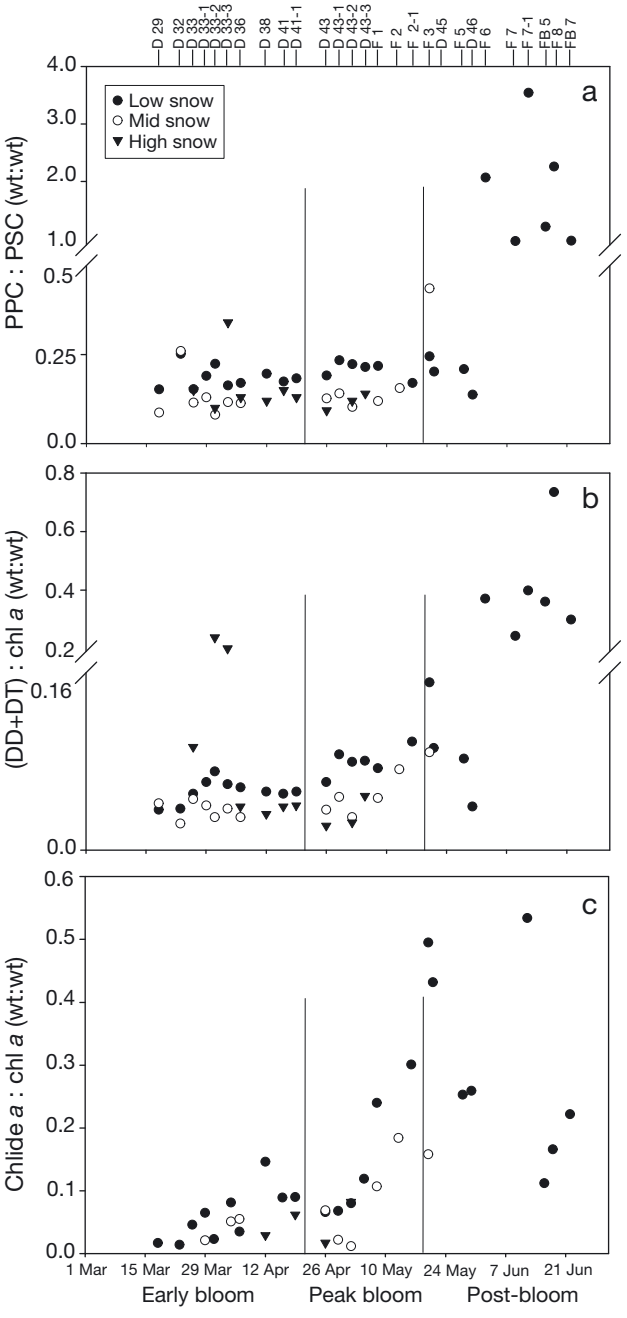

Fig. 7. Temporal changes in the ratios of (a) photoprotective (PPC) to photosynthetic carotenoids (PSC), (b) sum of diadinoxanthin and diatoxanthin (DD + DT) to chlorophyll *a* (chl *a*) and (c) chlorophyllide *a* (chlide *a*) to chl *a* under low, mid and high snow cover conditions. Sampling stations are indicated at the top of the upper panel

DT:(DD + DT), showed relatively constant values ranging from 0.16 to 0.26, with no significant differences across snow cover conditions (Kruskal-Wallis test, $p = 0.19$) or bloom periods (Kruskal-Wallis test, $p = 0.10$).

Degradation pigments

We identified 6 chlorophyll degradation products: chl *a* allomer and epimer, chlorophyllide *a*, monovinyl-chlorophyllide *a*, pheophorbide *a* and pheophytin *a*. Chl *a* allomers and epimers were at their minimum concentrations during the early bloom and peak bloom periods, and they increased during post-bloom. The sum of chl *a* allomer and epimer generally made up <15% of chl *a*, except for Stns D32, D33, D45, F3 and F5 which had greater values (maximum of 38% for Stn D32). The ratio of chl *a* allomer to chl *a* was significantly higher during the post-bloom (mean ± SD: 0.15 ± 0.06) compared to the early bloom (0.07 ± 0.03, Kruskal-Wallis test, $p < 0.05$). Chlorophyllide *a* (chlide *a*), which is frequently observed in senescent cells (Llewellyn et al. 2008), followed a similar trend to the allomers when normalized to chl *a*, with significantly higher values during the post-bloom period (Fig. 7c; Kruskal-Wallis test, $p < 0.05$).

Differences were also noted according to snow cover conditions. During the early bloom and peak bloom periods, concentrations of chlide *a* were generally higher under low snow cover conditions. For low snow cover conditions, the chlide *a*:chl *a* ratio was correlated with daily incident irradiance ($r_s = 0.50$, $p < 0.05$). The chl *a* allomer:chl *a* ratio also increased significantly with daily incident irradiance for low snow cover sites throughout all 3 bloom periods ($r_s = 0.72$, $p < 0.01$).

The increase of the chlide *a*:chl *a* ratio was accompanied by a greater percentage of large empty diatom cells during the post-bloom (Table 4; significant correlation between these variables: $r_s = 0.98$, $p < 0.05$). Although there was no significant relationship between these 2 variables during the early or peak bloom periods, both increased over time.

Pheophytin *a* was only present at 3 stations during the bloom period (maximum concentration: 4.1 mg m^{-2}). Pheophorbide *a* was more frequently observed, with a maximum pheophorbide *a*:chl *a* ratio of 0.97 (wt:wt), found at Stn D45 during the post-bloom. There were no significant differences for the pheophorbide *a*:chl *a* ratio throughout the different study periods or between different snow cover conditions. Although pheophorbide *a* and chlide *a* have been reported in association with senescent cells, there was no significant correlation between these pigments in the present study.

DISCUSSION

The present study showed that, aside from changes in algal composition that took place during the progression of the sea ice algal bloom during spring in the Arctic, sites that differed in terms of snow cover conditions also showed differences in terms of community composition as well as photoprotection, which highlights the important role of light in this environment.

Community composition

Diatoms dominated the sea ice algal bloom in both pigment and microscopic results, in agreement with past studies in the Arctic, with pennate diatoms contributing on average 68% of the abundance of sea ice eukaryote taxa in the Canadian Arctic (Poulin et al. 2011). The largest changes in the community composition occurred during the post-bloom, with increases in chlorophytes, prasinophytes, and dinoflagellates and a decrease in diatoms Type 2. However, this decrease was markedly observed only in a subset of stations (F6, F7, FB5, F8 and FB7). Since most of these stations were sampled near the end of the sampling (in June), they likely represent a later stage of the post-bloom.

The species succession described above is similar to that from other studies describing the Arctic bottom ice community. In general the community composition is characterized by the presence early in

Table 4. Mean (SD in parentheses) abundance of empty diatom cells relative to total number of cells and ratio of chlorophyllide *a* (chlide *a*) to chlorophyll *a* (chl *a*) during the early bloom (18 March to 19 April), peak bloom (26 April to 16 May) and post-bloom periods (20 May to 22 June); n: number of observations

Stage	Empty diatoms (%)	Chlide *a*:chl *a* (wt:wt)
Early bloom	11.5 (5.2)	0.07 (0.05)
	n = 6	n = 5
Peak bloom	16.2 (9.2)	0.20 (0.10)
	n = 10	n = 10
Post-bloom	36.2 (21.4)	0.33 (0.19)
	n = 5	n = 5

the season of flagellates along with a few solitary diatom species. As the season progresses the species composition changes to colony-forming pennate diatoms (such as *Nitzschia frigida*, *Navicula pelagica* and *Fragilariopsis cylindrus*), which dominate the community during the spring bloom period (Różańska et al. 2009). By the end of the bloom, in summer, diatoms are replaced with flagellates (Różańska et al. 2009, Mundy et al. 2011). In broad terms, this species succession is similar to the general pattern seen for pelagic environments (Margalef 1978).

Differences in community composition were observed for the various snow cover conditions, particularly in early bloom. These are thought to reflect different stages in the succession of species, influenced by the amount of light that reaches the bottom of the ice layer. The low irradiance, high snow cover conditions likely reflect an early stage of that succession, bearing some similarity with the low light conditions of early spring in that environment. Sites with these characteristics showed the presence of small flagellates such as prasinophytes and cryptophytes along with chlorophytes and 1 type of diatoms (Type 1) which gradually disappeared later on, whereas high irradiance, low snow cover sites were characterized by a significantly greater proportion of diatoms Type 2 (pennate diatoms). These observations match those from the study by Różańska et al. (2009) who showed a greater abundance of small flagellates under high snow conditions in the early bloom period (earlier in fact than the start of sampling during the present study), and more diatoms under low snow cover conditions. With the seasonal increase in irradiance in the present study (or a decrease in the snow cover during the early bloom and peak bloom periods), the community composition changed to pennate diatoms, followed by a gradual increase of dinoflagellates.

Photoprotective response

Sea ice algae cannot avoid exposure to excess irradiance by vertical displacement, as can, in a limited way, phytoplankton in the water column. Cells that perform in such an environment must be able to acclimate to the changes in irradiance (Petrou et al. 2011). Sudden changes can have major negative effects, as observed when the entire snow layer above the ice is removed experimentally, resulting in a decrease in algal biomass and growth rate (Juhl & Krembs 2010). In the present study, we examined *in situ* acclimation to the changing irradiances associated with different snow cover conditions. Our results show that, although generally dominant in sea ice, diatoms were favoured under low snow cover, higher relative irradiance conditions. This is not surprising as this algal group is recognized for its photoprotective performance, enabling cells to support wide variations in irradiance (Lavaud et al. 2004), including sea ice algae in Antarctica (Petrou et al. 2011). Our results show that the pool size of the xanthophyll-cycle pigments ([DD + DT]:chl *a*) or of all photoprotective pigments (PPC:chl *a* and PPC:PSC) increased significantly with increasing irradiance and was significantly higher under low snow cover. This response was observed with bottom ice irradiances as low as 26 µmol photons m^{-2} s^{-1} (early bloom, low snow cover conditions—compare with values <10 µmol photons m^{-2} s^{-1} for mid or high snow cover conditions at that time). There was little difference in photoprotective pigments between high and mid snow cover conditions, suggesting that the increase in irradiance observed under the mid snow cover conditions relative to high snow was not strong enough to elicit a photoprotective response in terms of pigments (high snow and mid snow cover bottom ice irradiances were, respectively, 4 and 9 µmol photons m^{-2} s^{-1} in early bloom and 7 and 13 µmol photons m^{-2} s^{-1} during peak bloom). Maximum values of (DD + DT):chl *a* were in the same range as for other polar regions (Kropuenske et al. 2009, Petrou et al. 2011), reaching a value of 0.40 (wt:wt) when irradiances were high. Values >0.40 have been suggested to occur during nutrient limitation for the Antarctic diatom *Chaetoceros brevis* (van de Poll et al. 2005, van de Poll & Buma 2009). The highest values of (DD + DT):chl *a* observed here were during post-bloom, and were also likely associated with nutrient limitation since nitrate concentrations were near zero during this period.

The fact that significantly greater concentrations of photoprotective pigments were found under low snow cover conditions further suggests that there was enough time for photoacclimation to take place and that it varied on small spatial scales since the different snow cover sites were within close proximity at each station. This implies that snow cover conditions remained relatively stable for several days. Juhl & Krembs (2010) estimated that the minimum acclimation time required by ice algae was on the order of 3 to 6 d, and, indeed, the best relationship that we observed between the PPC:PSC ratio and the daily bottom ice irradiance was when irradiance was averaged over the preceding 3 d (Fig. 8).

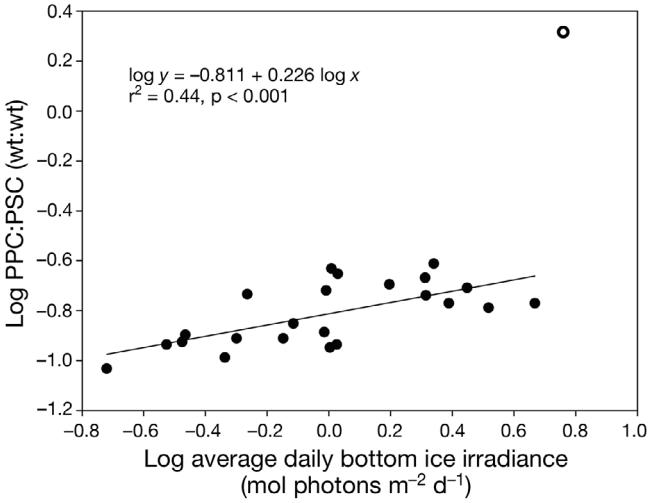

Fig. 8. Relationship between the ratio of photoprotective (PPC) to photosynthetic carotenoids (PSC) and average daily bottom ice irradiance (averaged over the preceding 3 d). One data point (white circle, Stn F6) was omitted to compute the regression. Note the log scale

The xanthophyll cycle is characterized by a fast (a few minutes) and a slow (acclimation) component (van de Poll & Buma 2009). Changes in the pool size (as above) belong to the latter. The fast component refers to the deepoxidation of diadinoxanthin into diatoxanthin. However, the usual sampling method by which sea ice is slowly melted in filtered seawater in darkness (>15 h) gives ample time for the back transformation of DT to DD. Indeed, there were no significant differences among snow covers for the deepoxidation index, DT:(DD + DT). The fact that this ratio remained at relatively high values (0.16 to 0.26) even though cells stayed in the dark for several hours during ice melting suggests that chlororespiration took place, inducing a proton gradient across the thylakoid membrane which favours the accumulation of DT (Jakob et al. 1999).

Physiological status of the cells

The physiological status of the cells (based on degradation products of chl *a*) differed according to the snow cover conditions during the early bloom and peak bloom periods. It also showed clear deterioration during the post-bloom period in late May to June. During the early bloom and peak bloom periods, pigments generally indicative of a deteriorating physiological condition (such as chlide *a* or the allomer of chl *a*) showed an increase under low snow cover conditions (higher relative irradiances) compared to the other snow covers. However, this was accompanied by increases in chl *a* biomass and in photoprotective pigments, suggesting rapid algal multiplication and adequate photoprotection rather than poor physiological health. Excess irradiance can harm cells, but small increases can be beneficial, as observed by Juhl & Krembs (2010) when only thin layers of snow were removed from the ice surface. Nutrient concentrations were low during early bloom (e.g. 2.0 to 3.7 µmol l^{-1} for nitrate) but not depleted, as found later during post-bloom. Hence, the presence of these chl *a* degradation pigments was perhaps related to the death and replacement of photosensitive species with phototolerant ones that were better photoprotected and growing faster (pennate diatoms). Other studies also observed the presence of chlide *a* during algal blooms, and various explanations have been proposed (e.g. cell autolysis; Llewellyn et al. 2008). Alternatively, changes in community composition under low snow cover could have favoured species showing high concentrations of chlide *a*, as seen for certain pennate diatoms (Quijano-Scheggia et al. 2008). In such a case, the presence of this pigment would be associated with a change in species rather than with poor physiological health.

During the post-bloom period, there were several indications of cell senescence as the diatom bloom declined, including the significant relationship of the chlide *a*:chl *a* ratio with the abundance of empty diatoms (Llewellyn et al. 2008). Algal senescence was likely related to nutrient depletion during post-bloom and possibly associated with high irradiances. The group of late-sampled stations mentioned above (F6, F7, FB5, F8 and FB7) showed fewer signs of senescence accompanied by strong photoprotection, suggesting that a transition had occurred to a community better acclimated to the low nutrient, high irradiance conditions.

The 2 pheopigments observed in our study (pheophytin *a* and pheophorbide *a*) showed no relationship to the algal senescence markers; therefore, we suggest that they were associated more with grazing than with a deteriorated physiological condition (Szymczak-Zyła et al. 2008). Copepod grazers were present in this environment (Wold et al. 2011), and Marquardt et al. (2011) reported the highest abundance of sympagic meiofauna in the bottom 3 cm of the ice during April and May of the same year. There were no significant differences in the concentration of pheophorbide *a* relative to chl *a* between snow cover conditions or between the different periods of the bloom, suggesting that grazing was not affected greatly by irradiance or bloom progression.

CONCLUSIONS

Using information on chemotaxonomic marker pigments in ice algae from the Beaufort Sea, we show that diatoms (pigment Type 2, pennates from microscopic observations) dominate the sea ice algal bloom during spring, followed by seasonal replacement with chlorophytes, prasinophytes and dinoflagellates during the post-bloom period. Snow cover conditions affected community composition only during the early bloom, when the low irradiance, high snow cover sites were characterized by the presence of diatoms Type 1 and chlorophytes which were not detected in the other snow cover sites. Higher relative irradiances under low snow cover conditions favoured the presence of diatoms Type 2 (pennate diatoms). We also observed significant differences in photoprotective pigments among the 3 snow cover conditions in early bloom, with enhanced photoprotection under low snow cover. This response, and the fact that the ratio of photoprotective to photosynthetic pigments was best correlated with the average bottom ice irradiance over the preceding 3 d, suggests that snow remained in place long enough for photoacclimation to take place. These conditions favoured the growth of sea ice algae, since the chl *a* biomass was greater under low snow cover conditions in the early bloom period. This was also associated with an increase in chl *a* degradation pigments possibly related to the presence of species with particularly abundant chlide *a* (possibly pennate diatoms). This study highlights the important role of light in controlling the algal communities in Arctic sea ice during spring, before the demise of the ice algal bloom. Extrapolation of our results to continued climate warming in the Arctic suggests that the ice algae spring bloom could benefit from a reduction of the snow cover (beneficial influence of light early on) but may be cut short by the shorter ice season.

Acknowledgements. This work is a contribution to the International Polar Year-Circumpolar Flaw Lead system study (IPY-CFL 2008), supported through grants from the Canadian IPY Federal Program office and the Natural Sciences and Engineering Research Council (NSERC) of Canada. E.A. received post-graduate scholarships from the Institut des sciences de la mer de Rimouski (ISMER) and Université du Québec à Rimouski and stipend from Québec-Océan. C.J.M. received a post-doctoral fellowship from Fonds québécois de la recherche sur la nature et les technologies. NSERC discovery grants to S.R. and to M.G. also helped to support this work. We are grateful to J. Gagnon for nutrient analysis, B. Philippe and S. Lessard for algal counts and identification, Dr. S. W. Wright for providing the CHEMTAX software, Dr. Papakyriakou for providing daily PAR data and Dr. J. K. Ehn for assisting with light attenuation calculations. We thank the officers and crew of the CCGS 'Amundsen' for logistical support and B. Philippe, M. Lionard and M. Simard for assistance in the field and/or laboratory. This is a contribution to the research programs of CFL, ISMER and Québec-Océan.

LITERATURE CITED

Alderkamp AC, de Baar HJW, Visser RJW, Arrigo KR (2010) Can photoinhibition control phytoplankton abundance in deeply mixed water columns of the Southern Ocean? Limnol Oceanogr 55:1248–1264

Arrigo KR, Mills MM, Kropuenske LR, van Dijken GL, Alderkamp AC, Robinson DH (2010) Photophysiology in two major Southern Ocean phytoplankton taxa: photosynthesis and growth of *Phaeocystis antarctica* and *Fragilariopsis cylindrus* under different irradiance levels. Integr Comp Biol 50:950–966

Ban A, Aikawa S, Hattori H, Sasaki H and others (2006) Comparative analysis of photosynthetic properties in ice algae and phytoplankton inhabiting Franklin Bay, the Canadian Arctic, with those in mesophilic diatoms during CASES 03-04. Polar Biosci 19:11–28

Barber DG, Asplin MG, Gratton Y, Lukovich J, Galley RJ, Raddatz RL, Leitch D (2010) The International Polar Year (IPY) Circumpolar Flaw Lead (CFL) system study: overview and the physical system. Atmos-Ocean 48:225–243

Belzile C, Johannessen SC, Gosselin M, Demers S, Miller WL (2000) Ultraviolet attenuation by dissolved and particulate constituents of first-year ice during late spring in an Arctic polynya. Limnol Oceanogr 45:1265–1273

Bidigare RR, Van Heukelem L, Trees CC (2005) Analysis of algal pigments by high-performance liquid chromatography. In: Andersen RA (ed) Algal culturing techniques. Elsevier Academic Press, Amsterdam, p 327–345

Brzezinski MA (1985) The Si:C:N ratio of marine diatoms: interspecific variability and the effect of some environmental variables. J Phycol 21:347–357

Garrison DL, Buck KR (1986) Organism losses during ice melting: a serious bias in sea ice community studies. Polar Biol 6:237–239

Grasshoff K, Kremling K, Ehrhardt M (1999) Methods of seawater analysis, 3rd edn. Wiley-VCH, New York, NY

Higgins HW, Wright SW, Schlüter L (2011) Quantitative interpretation of chemotaxonomic pigment data. In: Roy S, Llewellyn CA, Egeland ES, Johnsen G (eds) Phytoplankton pigments: characterization, chemotaxonomy and applications in oceanography. Cambridge University Press, Cambridge, p 257–301

Huner NPA, Öquist G, Sarhan F (1998) Energy balance and acclimation to light and cold. Trends Plant Sci 3:224–230

Ishikawa A, Wright SW, van den Enden R, Davidson AT, Marchant HJ (2002) Abundance, size structure and community composition of phytoplankton in the Southern Ocean in the austral summer 1999/2000. Polar Biosci 15: 11–26

Jakob T, Goss R, Wilhelm C (1999) Activation of diadinoxanthin de-epoxidase due to a chlororespiratory proton gradient in the dark in the diatom *Phaeodactylum tricornutum.* Plant Biol 1:76–82

Jeffrey SW (1997) Chlorophyll and carotenoids extinction coefficients. In: Jeffrey SW, Mantoura RFC, Wright SW (eds) Phytoplankton pigments in oceanography. UNES-

CO Publishing, Paris, p 595–596

Jeffrey SW, Wright SW, Zapata M (2011) Microalgal classes and their signature pigments. In: Roy S, Llewellyn CA, Egeland ES, Johnsen G (eds) Phytoplankton pigments: characterization, chemotaxonomy and applications in oceanography. Cambridge University Press, Cambridge, p 3–45

Juhl AR, Krembs C (2010) Effects of snow removal and algal photoacclimation on growth and export of ice algae. Polar Biol 33:1057–1065

Kozlowski WA, Deutschman D, Garibotti I, Trees CC, Vernet M (2011) An evaluation of the application of CHEMTAX to Antarctic coastal pigment data. Deep-Sea Res I 58: 350–364

Kropuenske LR, Mills MM, van Dijken GL, Bialey S, Robinson DH, Welschmeyer NA, Arrigo KR (2009) Photophysiology in two major Southern Ocean phytoplankton taxa: photoprotection in *Phaeocystis antarctica* and *Fragilariopsis cylindrus.* Limnol Oceanogr 54:1176–1196

Latasa M (2007) Improving estimations of phytoplankton class abundances using CHEMTAX. Mar Ecol Prog Ser 329:13–21

Lavaud J, Rousseau B, Etienne AL (2004) General features of photoprotection by energy dissipation in planktonic diatoms (Bacillariophyceae). J Phycol 40:130–137

Llewellyn CA, Tarran GA, Galliene CP, Cummings DG and others (2008) Microbial dynamics during the decline of a spring diatom bloom in the Northeast Atlantic. J Plankton Res 30:261–273

Mackey MD, Mackey DJ, Higgins HW, Wright SW (1996) CHEMTAX — a program for estimating class abundances from chemical markers: application to HPLC measurements of phytoplankton. Mar Ecol Prog Ser 144:265–283

Margalef R (1978) Life-forms of phytoplankton as survival alternatives in an unstable environment. Oceanol Acta 4: 493–509

Markus T, Stroeve JC, Miller J (2009) Recent changes in Arctic sea ice melt onset, freezeup, and melt season length. J Geophys Res 114:C12024, doi:10.1029/2009JC 005436

Marquardt M, Kramer M, Carnat G, Werner I (2011) Vertical distribution of sympagic meiofauna in sea ice in the Canadian Beaufort Sea. Polar Biol 34:1887–1900

Mundy CJ, Barber DG, Michel C (2005) Variability of snow and ice thermal, physical and optical properties pertinent to sea ice algae biomass during spring. J Mar Syst 58:107–120

Mundy CJ, Ehn JK, Barber DG, Michel C (2007) Influence of snow cover and algae on the spectral dependence of transmitted irradiance through Arctic landfast first-year sea ice. J Geophys Res 112:C03007, doi:10.1029/2006JC 003683

Mundy CJ, Gosselin M, Ehn JK, Belzile C and others (2011) Characteristics of two distinct high-light acclimated algal communities during advanced stages of sea ice melt. Polar Biol 34:1869–1886

NSIDC (National snow and ice data center) (2012) Arctic sea ice news & analysis. Available at: http://nsidc.org/arcticseaicenews/ (accessed 4 March 2012)

Perovich DK, Roesler CS, Pegau WS (1998) Variability in Arctic sea ice optical properties. J Geophys Res 103: 1193–1208

Petrou K, Ralph PJ (2011) Photosynthesis and net primary productivity in three Antarctic diatoms: possible significance for their distribution in the Antarctic marine ecosystem. Mar Ecol Prog Ser 437:27–40

Petrou K, Hill R, Doblin MA, McMinn A, Johnson R, Wright SW, Ralph PJ (2011) Photoprotection of sea-ice microalgal communities from the east Antarctic pack ice. J Phycol 47:77–86

Philippe B (in press) Changements récents dans la dynamique des algues de glace dans le secteur canadien de la mer de Beaufort. MSc thesis, Université du Québec à Rimouski

Poulin M, Daugbjerg N, Gradinger R, Ilyash L, Ratkova T, von Quillfeldt CH (2011) The pan-Arctic biodiversity of marine pelagic and sea-ice unicellular eukaryotes: a first-attempt assessment. Mar Biodiversity 41:13–28

Quijano-Scheggia S, Garcés E, Sampedro N, Van Lenning K and others (2008) Identification and characterization of the dominant *Pseudo-nitzschia* species (Bacillariophyceae) along the NE Spanish coast (Catalonia, NW Mediterranean). Sci Mar 72:343–359

Redfield AC, Ketchum BH, Richards FA (1963) The influence of organisms on the composition of sea-water. In: Hill MN (ed) The sea, Vol 2. Interscience, New York, NY, p 26–77

Rodriguez F, Varela M, Zapata M (2002) Phytoplankton assemblages in the Gerlache and Bransfield Straits (Antarctic Peninsula) determined by light microscopy and CHEMTAX analysis of HPLC pigment data. Deep-Sea Res II 49:723–747

Roy S, Mohovic B, Gianesella SMF, Schloss I, Ferrario M, Demers S (2006) Effects of enhanced UV-B on pigment-based phytoplankton biomass and composition of mesocosm-enclosed natural marine communities from three latitudes. Photochem Photobiol 82:909–922

Różańska M, Gosselin M, Poulin M, Viktor JM, Michel C (2009) Influence of environmental factors of the development of bottom ice protist communities during the winter–spring transition. Mar Ecol Prog Ser 386:43–59

Shannon CE (1948) A mathematical theory of communication. Bell Syst Technol J 27:379–423

Smith REH, Harrison WG, Harris LR, Herman AW (1990) Vertical fine structure of particulate matter and nutrients in sea ice of the high arctic. Can J Fish Aquat Sci 47: 1348–1355

Suzuki K, Minami C, Liu H, Saino T (2002) Temporal and spatial patterns of chemotaxonomic algal pigments in the subarctic Pacific and the Bering Sea during the early summer of 1999. Deep-Sea Res II 49:5685–5704

Szymczak-Zyła M, Kowalewska G, Louda JW (2008) The influence of microorganisms on chlorophyll *a* degradation in the marine environment. Limnol Oceanogr 53: 851–862

Tremblay JÉ, Bélanger S, Barber DG, Asplin M and others (2011) Climate forcing multiplies biological productivity in the coastal Arctic Ocean. Geophys Res Lett 38:LI8604, doi:10.1029/2011GL048825

van de Poll WH, Buma AGJ (2009) Does ultraviolet affect the xanthophyll cycle in marine phytoplankton? Photochem Photobiol Sci 8:1295–1301

van de Poll WH, von Leeuwe MA, Roggeveld J, Buma AGJ (2005) Nutrient limitation and high irradiance acclimation reduce PAR and UV-induced viability loss in the Antarctic diatom *Chaetoceros brevis* (Bacillariophyceae). J Phycol 41:840–850

Vidussi F, Roy S, Lovejoy C, Gammelgaard M and others (2004) Spatial and temporal variability of the phytoplankton community structure in the North water

Polynya, investigated using pigment biomarkers. Can J Fish Aquat Sci 61:2038–2052

Wold A, Darnis G, Søreide JE, Leu E and others (2011) Life strategy and diet of *Calanus glacialis* during the winter–spring transition in Amundsen Gulf, south-eastern Beaufort Sea. Polar Biol 34:1929–1946

Wright SW, Ishikawa A, Marchant HJ, Davidson AT, van den Enden RL, Nash G (2009) Composition and significance of picophytoplankton in Antarctic waters. Polar Biol 32:797–808

Wright SW, van den Enden RL, Pearce I, Davidson AT, Scott FJ, Westwood KJ (2010) Phytoplankton community structure and stocks in the Southern Ocean (30–80°E) determined by CHEMTAX analysis of HPLC pigment signatures. Deep-Sea Res II 57:758–778

Zapata M, Rodriguez F, Garrido JL (2000) Separation of chlorophylls and carotenoids from marine phytoplankton: a new HPLC method using a reversed phase C_8 column and pyridine-containing mobile phases. Mar Ecol Prog Ser 195:29–45

Editorial responsibility: Graham Savidge, Portaferry, UK

Submitted: March 7, 2012; Accepted: October 9, 2012
Proofs received from author(s): January 15, 2013